

The generation of martian floods by the melting of ground ice above dykes

Dan McKenzie & Francis Nimmo

Institute of Theoretical Geophysics, Bullard Laboratories, Department of Earth Sciences, University of Cambridge, Madingley Road, Cambridge CB3 0EZ, UK

The surface of Mars is cut by long linear faults with displacements of metres to kilometres, most of which are thought to have been formed by extension¹. The surface has also been modified by enormous floods, probably of water, which often flowed out of valleys formed by the largest of these faults². By analogy with structures on Earth^{3,4}, we propose here that the faults are in fact the surface expression of dykes⁵, and not of large-scale tectonic movements. We use a numerical model to show that the intrusion of large dykes can generate structures like Valles Marineris. Such dykes can provide a heat source to melt ground ice, and so provide a source of water for the floods that have been inferred to originate in some of the large valleys².

Most silica-rich bodies in the Solar System have reached their melting temperature at some stage in their history⁶, and the resulting surface features, such as volcanoes, lava flows and lava channels, have been mapped in some detail on Venus, Mercury, the Moon and Mars. There has been less interest in subsurface volcanic features, such as dykes⁷. On Earth, intrusive and extrusive volcanism generally occur together, and the same is likely to be true on other planets. The linearity and enormous horizontal extent of dykes on Earth is quite unlike structures produced by tectonic deformation. Terrestrial mafic dykes³ are up to 2,000 km long, with widths of 50–100 m and volumes of ~500 km³. They must be intruded in a few tens of days if the magma is not to solidify. When such an event occurs, a small collapse graben forms if the pressure of the magma is not sufficient for it to reach the surface. Depressions produced by the intrusion of small dykes have been mapped in Iceland⁸, where their surface expression is dominated by the presence of larger faults resulting from plate separation. On Venus, depressions associated with regional dykes produce surface roughness that is clearly visible on radar images^{7,9}, and can be followed for thousands of kilometres. Mège and Masson⁵ have proposed that similar features on Mars result from dyke intrusion. Though such graben have generally been mapped as tectonic features¹, their displacement–length ratios are much smaller than those of normal faults associated with tectonic extension¹⁰. When the same scales are used, maps of graben swarms

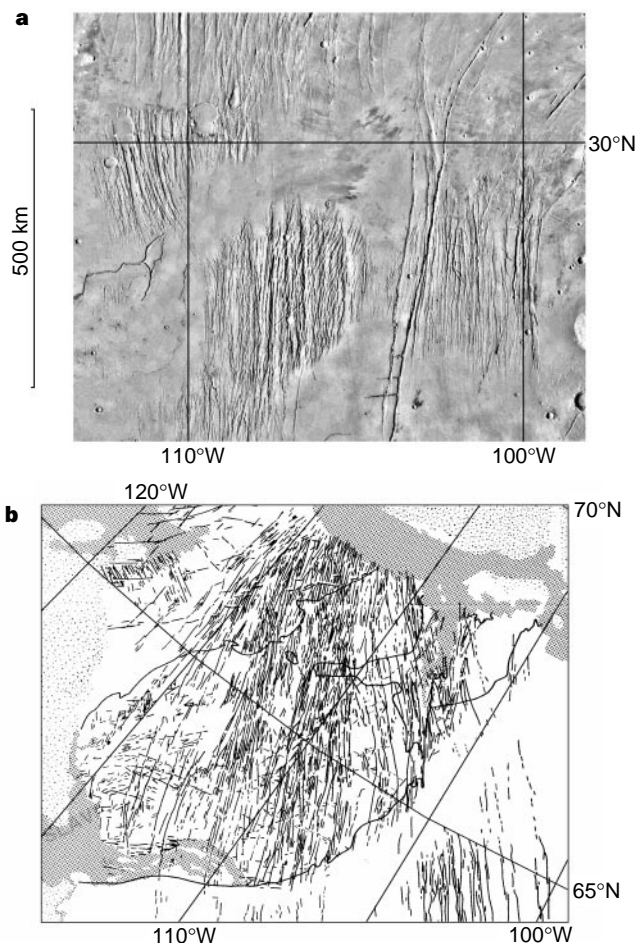


Figure 1 A comparison of graben swarms on Mars with dyke swarms on Earth. **a**, A mosaic of the northeastern portion of the Tharsis quadrangle (see Fig. 2a), showing graben swarms from several different generations of faulting (modified from USGS data available at <http://www.pdsimage.wr.usgs.gov/PDS/public/mapmaker/mapmkr.htm>). **b**, Part of the Mackenzie dyke swarm in northwest Canada (see Fig. 2b), based on ref. 4 and shown at the same scale as **a**. The boundaries of several metamorphic provinces of the Canadian Shield are also shown as wavy lines.

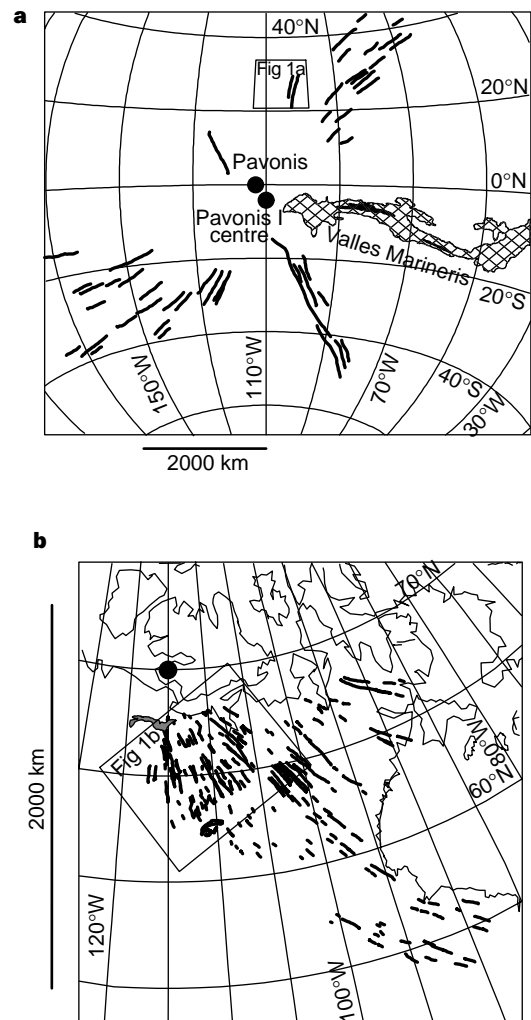


Figure 2 A comparison of two regions of Mars and Earth, both dominated by convective plumes. The large filled circles mark the likely positions of the plume centres that formed the radial structures. **a**, Azimuthal equidistant projection on 4°S, 110°W of fractures associated with the Pavonis I centre¹. **b**, Mackenzie dyke swarm⁴ using the same projection with centre 70°N, 115°W.

on Mars (Fig. 1a) closely resemble dyke swarms on Earth (Fig. 1b), though the longest graben on Mars (Fig. 2a) are about twice the length of the longest terrestrial dykes (Fig. 2b). On Earth, large dyke swarms—such as the Mackenzie swarm³ shown in Figs 1b and 2b—originate from the sites of plumes, where melt is produced by localized upwelling of hot mantle¹¹. On Mars, the large volcano Pavonis Mons, from which the graben in Fig. 2a radiate, has been constructed on top of the Tharsis bulge, which has the topographic and gravity anomalies expected from a large plume¹².

Plescia and Saunders¹ noticed that the Valles Marineris is radial to the Pavonis 1 centre in Fig. 2a. Therefore this large graben system may also be the surface expression of an enormous dyke. The cross-sectional area of the dyke modelled below is 350 km², and hence has a volume of 10⁶ km³ if its length is 3,000 km. The volume of one of the largest dykes on Earth, the Great Dyke of Zimbabwe¹³, is not likely to be greater than 5 × 10⁴ km³, or a factor of 20 smaller than that proposed for Mars. However, the volume of Olympus Mons on Mars is about a factor of 40 greater than that of Hawaii, the largest volcano on Earth, and the volume of melt produced by terrestrial plumes¹¹ is generally between 10⁶ and 10⁷ km³. The melt volume required by the model in Fig. 3 is therefore not unreasonably large. Like the features on Mars, the Great Dyke is associated with a number of parallel smaller dykes¹³. A large dyke could not only account for the linearity of Valles Marineris, but could also provide an explanation for the melting of ground ice which has produced the huge volumes of water that intermittently flooded out from the eastern end of this graben system to collect in the low-lying Chryse Planitia². Similar floods have flowed out of other valleys on Mars, such as Mangala Valles¹⁴, which also have graben at their probable

sources. Baker² has compared the features produced by these floods with the scablands of Washington State, USA, and has argued that the flow rates on Mars must have been ~2 × 10⁷ m³ s⁻¹, with a total volume of water of ~2,000 km³. In many places the margins of Valles Marineris consist of curved scarps. This morphology has been produced by mass wasting, which has caused the scarps to retreat from the large straight faults that bound the deeper parts of the troughs¹⁵. Masursky *et al.*¹⁶ argued that the scarp retreat was caused by the melting of a layer of ground ice, producing springs at the base of the escarpment that remove material and so cause landslides. They also suggested that the melting was caused by volcanism.

The processes involved in the transfer of volcanic heat to permafrost have received little attention¹⁷. The cooling of 1 kg of basalt from a temperature of 1,500 to 200 K releases enough heat to melt 5 kg of ice. Therefore a dyke 2,000 km long, 5 km deep and 50 m across, similar to one of the Mackenzie dykes, contains enough heat to produce 7,500 km³ of water. Hence there is no obvious energetic problem in generating the required volumes of water by dyke intrusion. We used a simple finite-difference model to discover whether the proposed mechanism could account for the general behaviour observed, rather than to model any individual feature. Figure 3 shows that intrusion of a dyke with a width of 16 km and a depth extent of 22 km, whose top is 9 km below the surface, produces a graben 26 km across and 6 km deep if the bounding faults dip at an angle of 60°. The base of the permafrost layer (5 km thick with an ice fraction of 0.2 by volume) first melts above the dyke. The melting zone spreads vertically and laterally with time, but never reaches the top of the frozen layer. At its greatest horizontal extent, the melt water extends over a width that is about twice that of the graben. Because the temperature is buffered at the melting point of ice until all the ice has melted, the surface temperature gradient remains low after dyke intrusion. Hence the melt water at the base of the permafrost does not start to refreeze until 8 Myr after the dyke is intruded. The vertical displacement on the faults which bound the graben is greater than the depth to the base of the permafrost, and melt water draining into the graben will lead to scarp retreat. In the absence of such draining, the pore pressure in the water will equal the weight of the overburden, because upward percolation is prevented by the permafrost. Regions underlain by such overpressured water are liable to large-scale catastrophic failure that produces a chaotic terrain like that commonly found on Mars¹⁵. The total volume of water generated reaches 6.5 km³ for each 1-km length of dyke 8 Myr after dyke intrusion. A 2,000-km-long dyke could therefore generate 1.3 × 10⁴ km³ of water. When the fraction of ice is 0.2, the subsidence caused by the melting is small compared to that produced by the dyke intrusion. Sills are also likely to occur on Mars, but would not produce any obvious surface expression. However, they would be at least as effective as dykes in melting ground ice.

It is difficult to model melting on Mars in detail, because the relevant parameters are poorly known. Estimates of the age of the floods², of 2–3 Gyr, are also uncertain, and depend on calibration of the cratering rate. The proportion of ice is unknown, though various estimates have been made¹⁸. The fraction could be as high as 1 in some depth intervals if frozen lakes are present. The thickness of the permafrost layer is controlled by the surface temperature gradient, and hence by the heat flux. Measurements of ¹⁴²Nd/¹⁴⁴Nd, ¹⁴³Nd/¹⁴⁴Nd, ¹⁷⁶Hf/¹⁷⁷Hf and ⁸⁷Sr/⁸⁶Sr in SNC (Shergotty–Nakhla–Chassigny) meteorites^{19,20} require the martian mantle to have been depleted in incompatible elements by melting within a few hundreds of Myr of its formation. This process transported almost all of the initial inventory of the heat-producing elements (K, U and Th) into the martian crust, where the isotopic constraints require them to have remained thereafter. Convective models of martian thermal evolution that are compatible with the geochemical observations suggest that heat flow from the mantle 2 Gyr ago was only

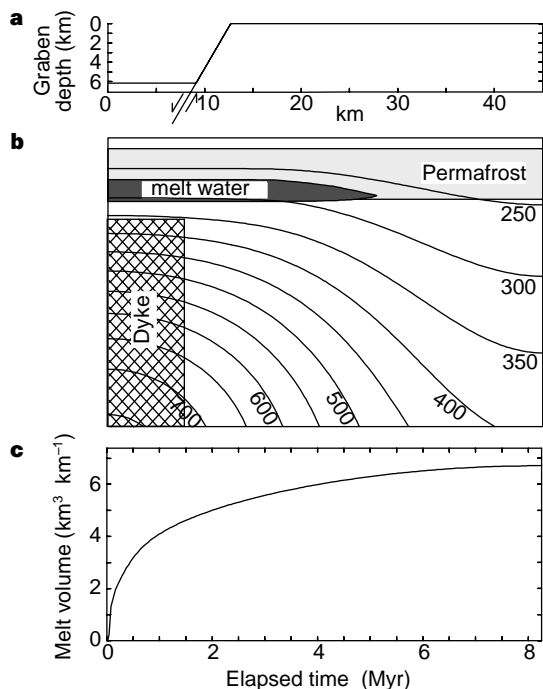


Figure 3 A numerical model of melting of ground ice by dyke intrusion. The calculation was performed using a rectangular box on a square mesh of 60 × 40, plotted with the same vertical and horizontal scales. The left- and right-hand sides of the box are mirror planes, the heat flux through the base is fixed at 16 mW m⁻², and the surface temperature is fixed at 200 K. The conductivity is 2 W m⁻¹ K⁻¹, the initial temperature of the dyke is 1,500 K, the latent heat of basalt is 560 kJ kg⁻¹, the specific heat is 1.2 kJ kg⁻¹ K⁻¹, and the fraction of ice present in the permafrost layer is 0.2. **a**, Cross-section of the surface graben, calculated by area conservation with fault dips of 60°. The faults start at the top corners of the dyke. Subsidence from melting is small and is neglected. **b**, Isotherms in K. **c**, Melt water volume per kilometre of dyke. After 8.25 Myr, the water starts to refreeze.

~16 mW m⁻², or less than half of that expected in the absence of geochemical differentiation¹². The surface temperature gradient depends on the integrated crustal radioactivity as well as the mantle heat flux, and may vary from 6 K km⁻¹ (where the crustal contribution is not important) to more than 20 K km⁻¹ (where it dominates). If the surface temperature is 200 K, the base of the permafrost is at a depth of between 11 and 3 km. Low geothermal gradients early in martian history are also suggested by geophysical estimates of the effective elastic thickness of more than 100 km beneath the Tharsis volcanoes²¹.

The large volumes of flood water that Baker² and Marsursky *et al.*¹⁶ propose to account for the observed landforms must have been released suddenly. The melting process modelled in Fig. 3 generates water far too slowly to maintain flow rates of 10⁷ m³ s⁻¹. The melt water must therefore first collect, either above or below the surface, before being suddenly released. Valles Marineris contains a number of closed depressions, some of which are dammed by large landslides. Such structures could collect water released from the subsurface, and are likely to undergo catastrophic failure, as they do on Earth.

The mass of water generated by the model in Fig. 3 is comparable to the total mass of the martian atmosphere. Spreading such a layer of water over a large part of Chryse Planitia might therefore have affected the surface temperature and humidity of the entire planet²². Most craters in Chryse Planitia show evidence of remobilization of ground ice²³. This discussion shows that there are no obvious problems with the proposed dyke model, which can account for graben such as Valles Marineris and which can produce the necessary volumes of water for the martian floods. If the above arguments are correct, only a few relatively minor structures on Mars, such as Thaumasia graben¹, have a purely tectonic origin. □

Received 28 January; accepted 19 October 1998.

1. Plescia, J. B. & Saunders, R. S. Tectonic history of the Tharsis Region, Mars. *J. Geophys. Res.* **87**, 9775–9791 (1982).
2. Baker, V. R. *The Channels of Mars* (Univ. Texas Press, Austin, 1982).
3. Fahrig, W. F. in *Mafic Dyke Swarms* (eds Halls, H. C. & Fahrig, W. F.) 331–348 (Spec. Pap. 34, Geol. Assoc. Canada, St John's, Newfoundland, 1987).
4. Fahrig, W. F. & West, T. D. Diabase dyke swarms of the Canadian Shield. (Map 1627A, Geol. Surv. Canada, Ottawa, 1986).
5. Mège, D. & Masson, P. A plume tectonics model for the Tharsis province, Mars. *Planet. Space Sci.* **44**, 1499–1546 (1996).
6. Basaltic Volcanism Study Project *Basaltic Volcanism on Terrestrial Planets* (Pergamon, New York, 1983).
7. Ernst, R. E., Head, J. W., Parfitt, E. A., Grosfils, E. & Wilson, L. Giant radiating dyke swarms on Earth and Venus. *Earth Sci. Rev.* **39**, 1–58 (1995).
8. Sigurdsson, O. Surface deformation of the Krafla fissure swarm in two rifting events. *J. Geophys. Res.* **47**, 154–159 (1980).
9. McKenzie, D., McKenzie, J. M. & Saunders, R. S. Dike emplacement on Venus and on Earth. *J. Geophys. Res.* **97**, 15977–15990 (1992).
10. Schultz, R. A. Displacement-length scaling for terrestrial and Martian faults: Implications for Valles Marineris and shallow planetary grabens. *J. Geophys. Res.* **102**, 12009–12015 (1997).
11. White, R. S. & McKenzie, D. Mantle plumes and flood basalts. *J. Geophys. Res.* **100**, 17543–17585 (1995).
12. Schubert, G., Solomon, S. C., Turcotte, D. L., Drake, M. J. & Sleep, N. H. in *Mars* (eds Kieffer, H. H., Jakosky, B. M., Snyder, C. W. & Matthews, M. S.) 147–183 (Univ. Arizona Press, Tucson, 1992).
13. Worst, B. G. The Great Dyke of Southern Rhodesia. *S. Rhodesia Geol. Surv. Bull.* **47**, (1960).
14. Zimbelman, J. R., Craddock, R. A., Greeley, R. & Kuzmin, R. O. Volatile history of Mangala Valles, Mars. *J. Geophys. Res.* **97**, 18309–18317 (1992).
15. Lucchitta, B. K. *et al.* in *Mars* (eds Kieffer, H. H., Jakosky, B. M., Snyder, C. W. & Matthews, M. S.) 453–492 (Univ. Arizona Press, Tucson, 1992).
16. Masursky, H., Boyce, J. M., Dial, A. L., Schaber, G. G. & Strobell, M. E. Classification and time of formation of Martian channels based on Viking data. *J. Geophys. Res.* **82**, 4016–4038 (1977).
17. Squyres, S. W., Wilhelms, D. E. & Moosman, A. C. Large-scale volcano-ground ice interaction on Mars. *Icarus* **70**, 385–408 (1987).
18. Squyres, S. W., Clifford, S. M., Kuzmin, R. O., Zimbelman, J. R. & Costard, F. M. in *Mars* (eds Kieffer, H. H., Jakosky, B. M., Snyder, C. W. & Matthews, M. S.) 523–556 (Univ. Arizona Press, Tucson, 1992).
19. Borg, L. E., Nyquist, L. E., Taylor, L. A., Wiesmann, H. & Shih, C.-Y. Constraints on Martian differentiation processes from Rb-Sr & Sm-Nd isotopic analyses of the basaltic Shergottite QUE94201. *Geochim. Cosmochim. Acta* **61**, 4915–4931 (1997).
20. Blichert-Toft, J. *et al.* Lu-Hf isotopic compositions of SNC meteorites: Implications of Martian mantle evolution. *Mineral. Mag.* **62**, 168–169 (1998).
21. Solomon, S. C. & Head, J. W. Heterogeneities in the thickness of the elastic lithosphere on Mars: Constraints on heat flow and internal dynamics. *J. Geophys. Res.* **95**, 11073–11083 (1990).
22. Baker, V. R. *et al.* Ancient oceans, ice sheets and the hydrological cycle on Mars. *Nature* **352**, 589–594 (1991).
23. Carr, M. H. *et al.* Martian impact craters and emplacement of ejecta by surface flow. *J. Geophys. Res.* **82**, 4055–4065 (1977).

Acknowledgements. We thank J. McKenzie for his help, and the Royal Society, Magdalene College, Cambridge, and NERC for support.

Correspondence and requests for materials should be addressed to F.N. (e-mail: nimmo@esc.cam.ac.uk).

Controlling the shape of a quantum wavefunction

T. C. Weinacht, J. Ahn & P. H. Bucksbaum

Department of Physics, University of Michigan, Ann Arbor, Michigan 48109-1120, USA

The ability to control the shape and motion of quantum states^{1,2} may lead to methods for bond-selective chemistry and novel quantum technologies, such as quantum computing. The classical coherence of laser light has been used to guide quantum systems into desired target states through interfering pathways^{3–5}. These experiments used the control of target properties—such as fluorescence from a dye solution⁶, the current in a semiconductor^{7,8} or the dissociation fraction of an excited molecule⁹—to infer control over the quantum state. Here we report a direct approach to coherent quantum control that allows us to actively manipulate the shape of an atomic electron's radial wavefunction. We use a computer-controlled laser to excite a coherent state in atomic caesium. The shape of the wavefunction is then measured¹⁰ and the information fed back into the laser control system, which reprograms the optical field. The process is iterated until the measured shape of the wavefunction matches that of a target wavepacket, established at the start of the experiment. We find that, using a variation of quantum holography¹¹ to reconstruct the measured wavefunction, the quantum state can be reshaped to match the target within two iterations of the feedback loop.

As in classical holography, quantum holography relies on interference between two waves, which can be labelled as 'object' and 'reference'. Whereas classical holography relies on classical light waves diffracting from scattering media, in quantum holography the object and reference are combined in a single coherently prepared quantum state. This state is a superposition of a shaped wavepacket (the 'object') and a reference wavepacket (the 'signal'). The object and reference packets are created by two specially shaped coherent laser pulses with a time delay, τ , between them. The interference between the object and the reference modulates the spectrum of the wavefunction. A careful measurement of this interference and how it changes with the time delay τ can be used to reconstruct the object wavefunction¹⁰. This is similar to the optical technique known as spectral interferometry, which is used to determine the phase and amplitude of a classical light pulse^{12,13}.

The essential feature in our application of quantum holography is the ability to measure independently the amplitude of each state in the total wavepacket. This is accomplished with state selective field ionization (SSFI)¹⁴. SSFI allows us to project the total wavefunction onto the eigenstates of the atomic hamiltonian and directly measure the amplitude of each projection. Eigenstate signals indicate the amplitude of each state in the wavepacket. The correlations in fluctuations of pairs of states indicate the relative phase difference between two states in the object wavepacket and their corresponding states in the reference packet^{15,16}. The measured phase and amplitude of each state can be used to reconstruct the object wavepacket as a coherent superposition of eigenstates^{17–20}. In the work reported here, this measurement was used as feedback to reshape the optical excitation pulse and thereby reshape the wavepacket.

Both the signal and reference wavepackets were created by irradiating an effusive beam of prepared caesium atoms with two ultrafast, broadband light pulses from an amplified titanium sapphire laser system. The atoms were prepared in the 7s state from the 6s ground state via a two-photon transition driven by an intense nanosecond dye-laser pulse with a wavelength of 1.08 μm . The ultrafast pulses excited a small portion of the electronic wavefunc-